Enhanced Prediction of the Flexural Capacity of Prestressed Reinforced Concrete Beams Using an Improved PSO-ANN Model

Thu Minh Tran
Faculty of Civil Engineering, University of Transport and Communications, Hanoi, Vietnam
minhtran250999@gmail.com (corresponding author)

Ha Linh Le
Faculty of Civil Engineering, University of Transport and Communications, Hanoi, Vietnam
lhlinh@utc.edu.vn

Received: 24 October 2025 | Revised: 26 November 2025 and 8 December 2025 | Accepted: 10 December 2025

 DOI: https://doi.org/10.48084/etasr.15746

ABSTRACT

Accurate prediction of the flexural capacity of Prestressed Reinforced Concrete (PRC) beams remains a complex task due to nonlinear interactions among mechanical properties, environmental influences, and deterioration mechanisms such as corrosion and sustained loading. This study proposes a novel hybrid prediction framework that integrates an Improved Particle Swarm Optimization (IPSO) algorithm with an Artificial Neural Network (ANN) to enhance predictive performance in both accuracy and computational efficiency. The key innovation lies in the IPSO algorithm, which employs adaptive inertia weights and dynamic acceleration coefficients to effectively balance global exploration and local exploitation during training, thereby accelerating convergence and preventing premature convergence to local optima. To ensure model robustness, a unique dataset was synthetically generated using Monte Carlo simulations to reflect realistic variability in critical factors, including load levels, corrosion ratios, concrete strength, temperature, and humidity, based on actual experimental configurations. The proposed IPSO-ANN model significantly outperformed baseline models (standard PSO-ANN and Adam-ANN), as demonstrated by its superior results in Mean Squared Error (MSE), Mean Absolute Error (MAE), Root Mean Squared Error (RMSE), and the coefficient of determination (R^2). Moreover, it achieved a notable reduction in computation time compared to the standard PSO, highlighting the algorithm's efficiency.

Keywords-capacity; prestressed reinforced concrete; Particle Swarm Optimization (PSO); artificial neural networks

I. INTRODUCTION

PRC beams are widely used in bridges and buildings due to their superior flexural strength, durability, and serviceability performance [1-4]. Numerous analytical and numerical approaches have been developed to estimate their flexural capacity under various loading and environmental conditions. Authors in [5] developed a refined layered-section analysis, incorporating a modified CEB–FIP creep model with steel fiber effects, to predict long-term deflection and assess the serviceability reliability of compression-yielding FRP-reinforced concrete beams. Authors in [6] evaluated the flexural strengthening and post-damage rehabilitation of reinforced concrete beams using externally bonded low- and high-density BFRP sheets, supported by both experiments on two-span beams and finite element analysis.

However, most conventional analytical models rely on simplified mechanical assumptions and deterministic parameters, which may not accurately represent the nonlinear response and degradation mechanisms of real structures.

Design standards, such as Eurocode 2 [7], provide general design principles for prestressed concrete members, yet their predictive capability is limited when accounting for material variability, prestress losses, and other uncertainties that evolve over time. The analytical study in [8] and the nonlinear modeling framework in [9] have advanced the understanding of flexural behavior and seismic assessment of prestressed concrete. Nevertheless, these traditional approaches remain dependent on fixed input parameters and cannot efficiently adapt to complex data or probabilistic conditions.

To overcome such limitations, researchers have incorporated computational and data-driven techniques into structural analysis. Authors in [10] proposed a unified classical and matrix framework for the structural analysis of prestressed concrete, which provides a robust theoretical foundation for hybrid modeling. Authors in [11] reviewed deep learning-based

methods for structural health monitoring and demonstrated the potential of neural architecture to learn nonlinear patterns from large-scale sensor data. Similarly, authors in [12] presented a nonlinear and time-dependent analytical model for continuous unbonded prestressed concrete beams, highlighting the significant effect of rheological and creep behaviors on long-term flexural performance.

Despite these advances, the combined application of intelligent optimization and ANNs [13-15] for predicting PRC beam flexural capacity remains limited. AI-driven research on structural safety and scour prediction further underscores the potential of hybrid metaheuristic–neural approaches [16-19] to address complex structural problems. Motivated by these developments, the present study proposes an IPSO-ANN model for enhanced and more reliable prediction of the flexural capacity of PRC beams.

While previous studies have advanced the analysis and design of reinforced concrete and PRC beams, most conventional analytical models still rely on simplified mechanical assumptions and deterministic parameters, which limit their ability to represent the nonlinear degradation induced by corrosion, sustained loading, and environmental actions. Several AI-based approaches, including ANN, ANFIS, and hybrid metaheuristic–neural models, have been proposed to predict the flexural capacity of corroded or strengthened concrete beams, and they generally outperform code-based formulas and classical regression models [20-23]. However, these studies typically consider a more limited set of influencing parameters and rarely incorporate the combined effects of sustained load level, corrosion damage, concrete strength, temperature, and humidity, nor do they employ an improved PSO scheme tailored to probabilistic datasets generated via Monte Carlo simulation.

The present work addresses these gaps by developing an IPSO–ANN framework specifically for predicting the flexural capacity of PRC beams. The proposed model integrates an IPSO algorithm with an ANN to enhance global search capability and convergence, and it is trained on a Monte Carlo–generated dataset calibrated to experimental PRC beam tests, capturing realistic variability in load level, degree of corrosion, material properties, and environmental conditions. The IPSO–ANN framework achieves a higher coefficient of determination (R^2 = 0.945 versus R^2 = 0.940 for Adam) and improved computational efficiency compared with the baseline optimization schemes, providing a more reliable and robust tool for flexural capacity prediction of PRC beams under combined mechanical and environmental actions.

II. MATERIALS AND METHODS

A. Data Generation Using Monte Carlo Simulations

This study involved the casting and testing of six PRC beams designed to investigate the effects of sustained loads and corrosion. The beams were constructed in two stages: the initial casting utilized C40 concrete with a height of 350 mm, as shown in Figure 1, followed 18 days later by an additional top layer of C45 concrete, 100 mm thick, simulating a reinforced concrete floor system [24].

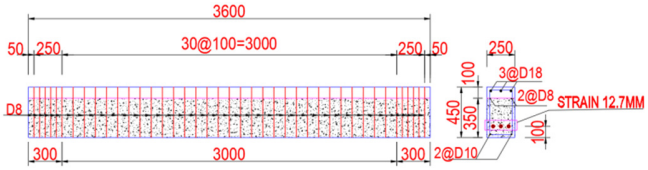

Fig. 1. Experimental beam dimensions.

The reinforcement configuration included HRB400 rebars with a diameter of 18 mm at the top of the beams, along with HRB335 rebars of 8 mm and 10 mm diameter used for structural support and stirrups. Stirrups, made of HRB335 steel with an 8 mm diameter, were spaced at 50 mm intervals near the beam ends and 100 mm in other regions.

The beams with a 3D view, as depicted in Figure 2, were prestressed using the pre-tensioning method with three low-relaxation steel strands of 12.7 mm diameter, positioned 67 mm above their bottom. These strands, with a nominal strength of f_{ptk} = 1860 MPa, were tensioned to 1398 MPa (approximately 75% of the ultimate strength), corresponding to a total initial prestressing force of 414 kN, prior to the initial casting. After nine days, prestress transfer was achieved through controlled relaxation. It is acknowledged that the initial prestressing force decreases due to instantaneous losses (elastic shortening) and time-dependent losses (creep, shrinkage, and steel relaxation). In this study, the effective prestress (f_{pe}) at the time of testing was evaluated in accordance with design standards, ensuring that the input parameters for the simulation reflect the actual state of the beams after losses have occurred. The six beams were subjected to transverse concentrated sustained loads (P) of 0, 50, and 100 kN, applied at the mid-span of the beams. These loads represent approximately 0%, 30%, and 60% of the design ultimate bearing capacity, respectively. Corrosion conditions varied, with beams exposed to both corroding and non-corroding environments. Material properties for both concrete and steel were evaluated following the Chinese material testing standard GB/T 50152-2012: Standard for testing methods of concrete structures (Standardization Administration of China, 2012) [25]. The detailed experimental configuration and the corresponding ultimate load capacity (P_u) obtained from the tests are summarized in Table I.

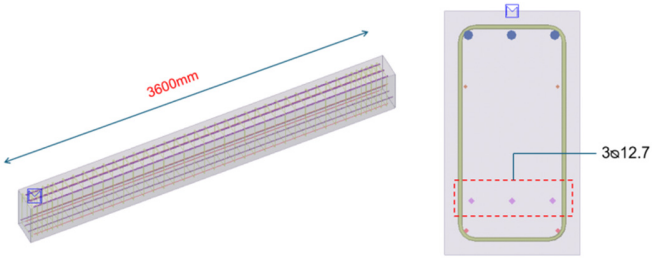

Fig. 2. 3D view of experimental beam.

TABLE I. EXPERIMENTAL CONFIGURATION AND LOAD CAPACITY

Beam ID	Sustained load P (kN)	Corrosion status	Concrete strength f'_c (MPa)	Ultimate load P_u (kN)
B1	0.0	Non-corroded	55.4	168.5
B2	50	Non-corroded	54.2	162.3
B3	100	Non-corroded	53.8	108.7
B4	0.0	Corroded	54.5	105.4
B5	50	Corroded	52.6	55.2
B6	100	Corroded	53.1	48.90

Given that six experimental data points are insufficient for training deep neural networks, a data augmentation strategy using Monte Carlo simulations was conducted to generate a robust dataset of 1,000 samples [27]. The experimental results from the six beams served as the baseline input parameters. Specifically, the tested concrete strength and applied load levels defined the statistical means and discrete peaks for the simulation distributions. Probability distributions were then assigned to these parameters (e.g., Normal distribution for concrete strength, Uniform distribution for environmental factors) to reflect realistic material and environmental variability. This hybrid approach ensures that the synthetic dataset is statistically significant while remaining physically grounded in the experimental observation [26]. The following key parameters were simulated:

- The distribution of sustained load (P) is concentrated at three distinct levels: 0, 50, and 100 kN, indicating a structured approach to analyzing specific load states.
- The corrosion ratio (h) shows peaks at 27.5% and 30%, suggesting controlled experimental conditions at fixed levels.
- Concrete strength (f'_c) is evenly distributed between 52 and 56 MPa, ensuring unbiased data for durability analysis.
- Temperature (T) spans from 0°C to 35°C with a nearly uniform distribution, capturing diverse environmental conditions.
- Relative humidity (RH) varies between 50% and 100%, reflecting significant environmental variability that may influence material properties.

The synthetic dataset consisted of 1,000 samples for each parameter, enabling comprehensive analysis of parameter impacts. The variability introduced through these simulations ensures robustness and applicability to diverse real-world scenarios.

Figure 3 illustrates the statistical distributions of the five input parameters used for generating the synthetic dataset utilizing Monte Carlo simulations: sustained load (P), corrosion ratio (h), concrete compressive strength (f_s), temperature (T), and relative humidity (RH). The sustained load exhibits a discrete distribution with three dominant peaks at 0, 50, and 100 kN, corresponding to the predefined loading levels in the experimental setup. This structured distribution enables focused assessment of the effects of load magnitude on beam behavior.

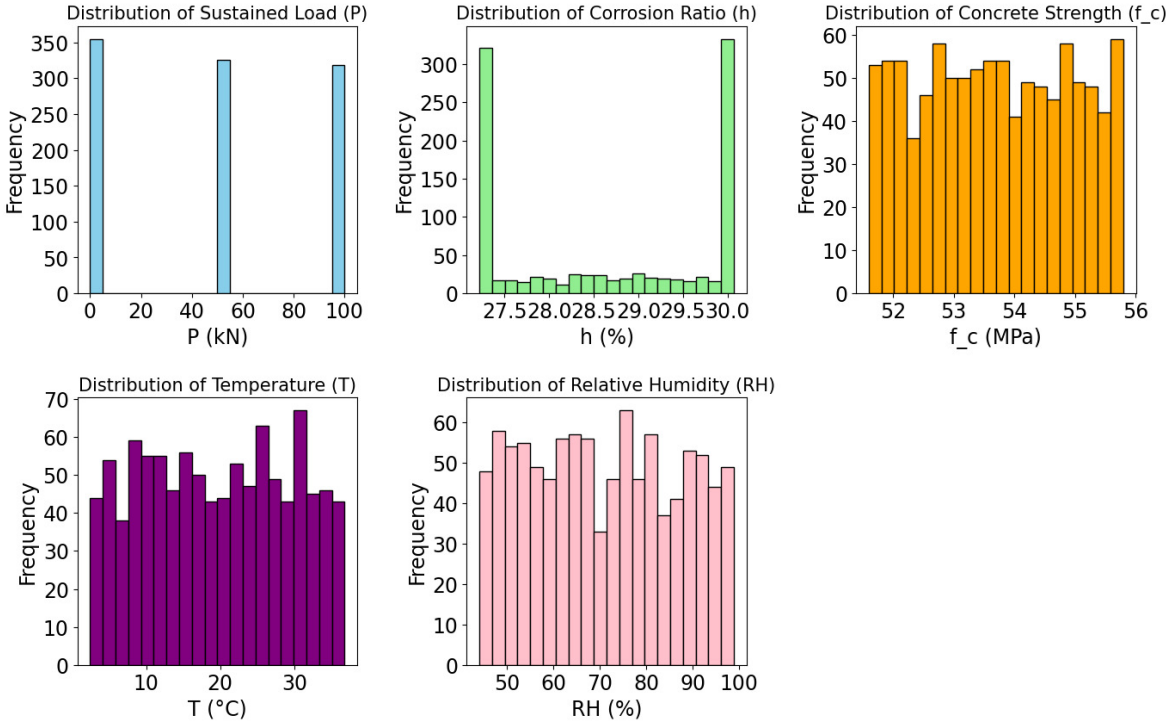

Fig. 3. Input variable distribution chart.

The corrosion ratio displays a left-skewed distribution concentrated between 27.5% and 30%, reflecting controlled simulation of corrosion scenarios. The distribution of concrete compressive strength follows an approximately normal pattern centered around 53–54 MPa, capturing natural material variability and ensuring a realistic representation of concrete performance. In contrast, temperature and relative humidity are distributed nearly uniformly over the ranges of 0–40°C and 50%–100%, respectively. These broad, non-biased environmental ranges are intended to encompass diverse climatic conditions, thereby enhancing the generalizability and robustness of the proposed IPSO-ANN model.

B. Artificial Neural Networks

ANNs are computational models, inspired by the neural architecture of the human brain, and are widely utilized for modeling highly nonlinear relationships. In this study, ANNs are used to predict the flexural capacity of PRC beams by learning patterns from the data generated through Monte Carlo simulations. The ANN model consists of an input layer, multiple hidden layers, and an output layer. Each layer comprises neurons, which relate to adjustable weights and biases. An ANN consists of the following main components:

- Input Layer: The input layer includes nodes representing the key parameters influencing flexural capacity, such as sustained load, corrosion ratio, concrete strength, temperature, and humidity.
- Hidden Layers: One or many hidden layers are employed, with each layer containing a fixed number of neurons optimized through iterative testing. Activation functions, such as ReLU, are applied to introduce nonlinearity and capture complex relationships.
- Output Layer: The output layer consists of a single neuron, representing the predicted ultimate flexural load (P_u) of the beam (in kN).

C. Proposed Predictive Method

The proposed IPSO-ANN framework integrates the IPSO algorithm with ANNs to enhance predictive performance. IPSO optimizes the ANN's weights and biases dynamically, improving convergence speed, accuracy, and robustness. The IPSO algorithm refines the standard PSO with adaptive inertia weight (w) and dynamic acceleration coefficients (c_1 and c_2), addressing the trade-off between exploration (global search) and exploitation (local search).

a) Velocity Update Equation

$$v_i^{k+1} = w \cdot v_i^k + c_1 \cdot r_1 \cdot \left(p\ Best_i - x_i^k\right) + c_2 \cdot r_2 \cdot \left(g\ Best - x_i^k\right) \quad (1)$$

where v_i^{k+1} is the velocity of the particle i at iteration $k+1$; w is the adaptive inertia weight; c_1 and c_2 are the cognitive and social coefficients, respectively; r_1 and r_2 are Random numbers uniformly distributed between [0, 1]; $p\ Best_i$ is the best position of particle I; $g\ Best$ is the global best position; and x_i^k is the current position of particle i.

b) Position Update Equation

$$x_i^{k+1} = x_i^k + v_i^{k+1} \quad (2)$$

c) Adaptive Inertia Weight

$$w = w_{max} - \left(\frac{w_{max} - w_{min}}{iter_{max}}\right) \cdot\ iter \quad (3)$$

where w_{max} and w_{min} are maximum and minimum inertia weights, respectively; $iter_{max}$ is the maximum number of iterations; and $iter$ is the current iteration.

The IPSO algorithm is used to optimize ANN parameters (weights and biases), encoded as particles in the search space. The process involves:

$$Particle = \left[w_{1,1}, w_{1,2}, \ldots . w_{m,n}, b_1, b_2\ \ldots, b_m\right] \quad (4)$$

where $w_{n,m}$ is the weight connecting the neuron n in one layer to the neuron m in the next layer and b_m is the Bias of the neuron m.

$$\text{Fitness } = \frac{1}{N}\sum_{i=1}^{N} (y_i - \hat{y}_i)^2 \quad (5)$$

where N is the number of data samples, y_i is the true output, and $\hat{y}_i$ is the predicted output.

III. RESULTS AND DISCUSSION

The performance of ANN models was optimized using three algorithms: PSO, Adam, and IPSO. By analyzing predicted and true values, residual distribution, and key performance metrics, the present study highlights the differences in prediction accuracy, computational efficiency, and model stability between the three optimization strategies. Figure 4 compares the predicted and true values obtained using ANN models optimized with PSO, Adam, and IPSO, demonstrating significant differences in prediction performance across these methods. Both PSO and IPSO achieve high performance, with predicted values closely clustered around the ideal line, indicating strong data fitting capability. IPSO stands out with higher accuracy, as its data points are distributed closer to the ideal line, minimizing deviation from the actual values. In contrast, the Adam algorithm shows a wider dispersion of data compared to PSO and IPSO, with many data points being farther from the ideal line. This indicates that Adam struggles to optimize model parameters to achieve the same prediction accuracy as the other two methods. These results confirm IPSO's superior effectiveness in improving prediction accuracy and highlight the advantage of swarm-based optimization algorithms (PSO and IPSO) in training ANNs over Adam. The results of the residuals and predicted plot analysis, as displayed in Figure 5, reveal significant differences in performance between the methods. The PSO and IPSO methods exhibit a relatively uniform distribution of residuals around the zero residual line, indicating stable predictive capabilities and reduced errors. IPSO demonstrates superior performance with a more stable residual distribution and fewer outliers compared to PSO, highlighting the algorithm's improved efficiency. In contrast, the Adam method shows greater residual dispersion and the presence of more outliers, indicating poorer prediction performance and higher sensitivity to the data.

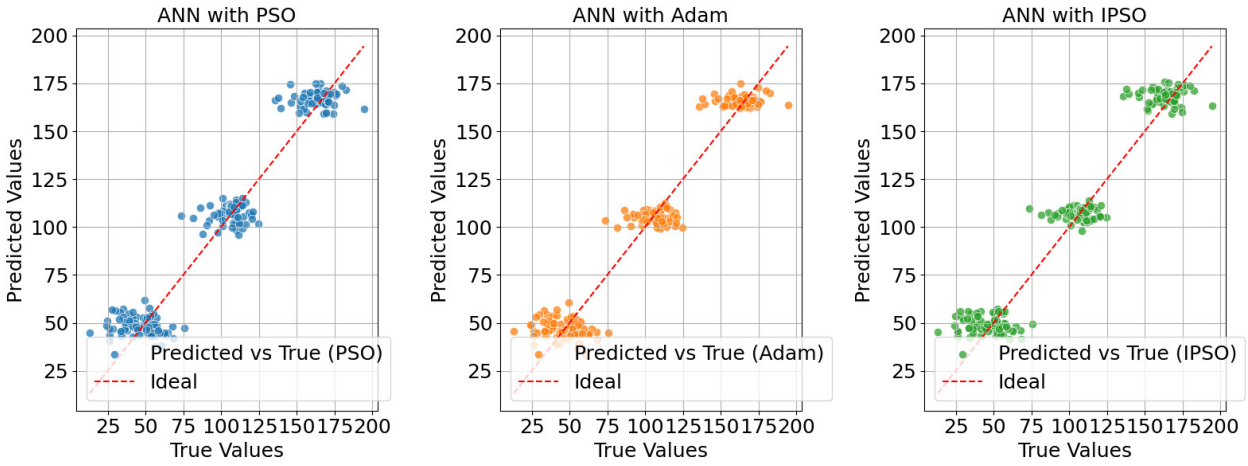

Fig. 4. Comparison of predicted and true values for ANN models with PSO, Adam, and IPSO.

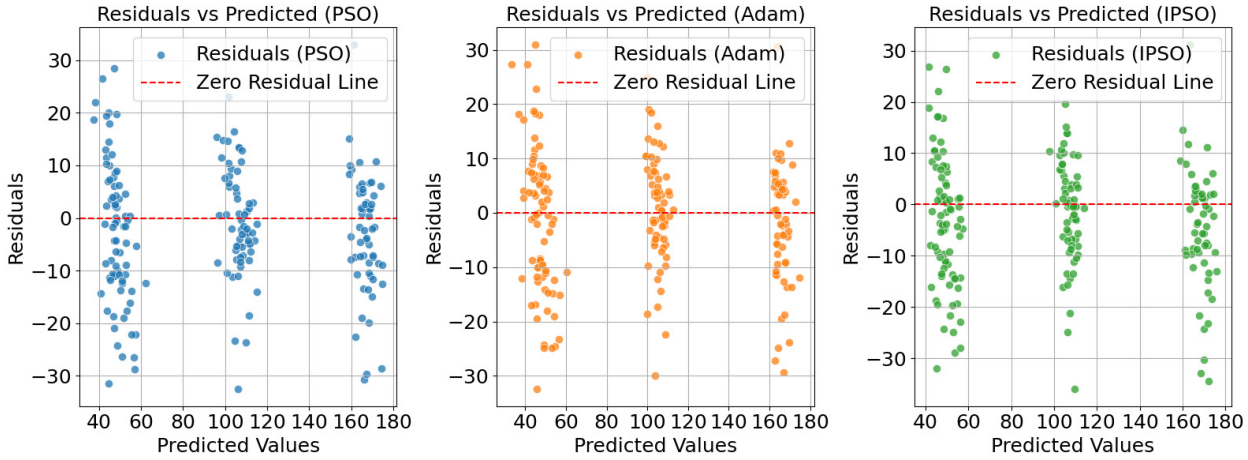

Fig. 5. Residuals and predicted values for ANN models with PSO, Adam, and IPSO.

The evaluation of predictive performance metrics provides a quantitative comparison of the three optimization algorithms: Adam, PSO, and IPSO, which are used in training ANN models. The metrics include MSE, MAE, RMSE, and R^2 and collectively assess the model accuracy, error magnitude, and explanatory power. Table II outlines the performance of each model.

TABLE II. PERFORMANCE METRICS' COMPARISON FOR ANN MODELS WITH ADAM, PSO, AND IPSO

Metric	ANN with Adam	ANN with PSO	ANN with IPSO
MSE	139.76	145.25	132.86
MAE	9.26	9.44	9.06
RMSE	11.82	12.05	11.52
R^2	0.943	0.940	0.945

The evaluation of the ANN models using PSO, Adam, and IPSO optimization algorithms reveals: (i) that IPSO consistently outperforms other algorithms across all metrics. IPSO achieves the lowest errors with an MSE of 132.86, MAE of 9.06, and RMSE of 11.53, along with the highest explanatory power (R^2 = 0.9459), demonstrating its superior optimization capability and predictive accuracy. PSO performs moderately, showing lower errors and higher explanatory power (R^2 = 0.9431) than Adam but still falling short of IPSO. Adam ranks the lowest, with the highest MSE (145.25), MAE (9.45), and RMSE (12.05), and the lowest R^2 (0.9409), indicating relatively weaker predictive performance. These results emphasize IPSO's effectiveness in minimizing prediction errors and enhancing model performance.

In addition to prediction accuracy, computation time is a critical factor in evaluating optimization algorithms. Table II compares the computational efficiency of Adam, PSO, and IPSO algorithms, highlighting the trade-offs between speed and optimization performance.

As presented in Table III, the fastest computation time (24.08 s) is achieved using the Adam algorithm, a gradient-based optimization method known for its ability to store momentum and decay rates. This helps minimize computational costs. However, the Adam-optimized model often fails to fully explore the search space, particularly in complex nonlinear problems, as compared to PSO or IPSO. In contrast, the ANN combined with PSO requires significantly

more computation time (199.47 s) due to PSO's nature as a population-based algorithm. PSO processes multiple particles simultaneously, and each particle evaluates its fitness value (loss) over several iterations. This greatly increases computational costs, especially when the number of particles or iterations is high. The ANN combined with IPSO improves computation time compared to PSO, taking only 194.25 s, a reduction of approximately 2.6%. This improvement is attributed to IPSO's use of adaptive inertia weights, which better balance exploitation and exploration. As a result, IPSO reduces unnecessary updates in the search space, and its particles tend to converge faster toward potential optimal regions, thereby lowering computational costs.

TABLE III. COMPUTATION TIME COMPARISON FOR ANN MODELS WITH ADAM, PSO, AND IPSO

Algorithm	Computation time (s)
ANN with Adam	24.08
ANN with PSO	199.47
ANN with IPSO	194.25

Compared with previous ANN, ANFIS, and PINN-based models, developed for predicting the flexural response of corroded or lightweight reinforced concrete beams [20-23], the proposed IPSO–ANN framework presents several distinctive features. Most existing studies focus on conventional corroded reinforced concrete beams without prestressing or on lightweight reinforced concrete beams, while they do not simultaneously account for sustained loading and environmental variability. In contrast, the present work explicitly addresses PRC beams and incorporates sustained load level, degree of corrosion, concrete strength, ambient temperature, and relative humidity in a unified predictive model.

In addition, earlier AI-based approaches usually employ standard gradient-based or evolutionary training schemes and are often constrained by relatively small experimental datasets. In the present study, the IPSO algorithm introduces adaptive inertia weights and dynamic acceleration coefficients to improve the exploration–exploitation balance, and the ANN is trained on an extensive Monte Carlo–generated dataset calibrated to experimental PRC beam tests. According to the obtained results, the IPSO–ANN model attains the highest R^2 and the lowest error metrics among the optimization schemes investigated, while explicitly addressing a more complex and practically relevant set of influencing parameters for PRC beams.

IV. CONCLUSIONS

This study presents a robust framework for predicting the flexural capacity of Prestressed Reinforced Concrete (PRC) beams using an Improved Particle Swarm Optimization (IPSO) algorithm integrated with Artificial Neural Networks (ANNs). The key conclusions are:

- The IPSO-ANN model demonstrated superior accuracy and efficiency compared to conventional PSO and Adam-optimized ANN models. Metrics such as Mean Squared Error (MSE), Mean Absolute Error (MAE), Root Mean Squared Error (RMSE), and coefficient of determination (R^2) consistently highlighted the IPSO model's ability to minimize prediction errors and accurately capture nonlinear relationships.
- The IPSO algorithm's adaptive inertia weight and dynamic parameter adjustment contributed to faster convergence and better exploration of the solution space. This ensures stability and robustness in diverse and complex prediction scenarios.
- The integration of Monte Carlo simulations allowed for comprehensive data generation, reflecting real-world variability in factors such as sustained load, corrosion ratio, and environmental conditions. This highlights the practical relevance of the proposed approach for structural health monitoring and design optimization.
- While Adam offered faster computation times, its lower prediction accuracy underscores the importance of selecting optimization methods tailored to the complexity of the problem. PSO and IPSO, despite their higher computational costs, provided significantly better prediction outcomes, with IPSO achieving a balance between performance and efficiency.

The results of this study underscore the potential of combining advanced optimization techniques with machine learning to address challenges in structural engineering. By advancing predictive capabilities, the proposed IPSO-ANN model offers a reliable tool for engineers and researchers, facilitating informed decision-making in the design and maintenance of PRC structures. Future research could explore the application of this approach to other structural elements and further refine optimization strategies for enhanced computational efficiency.

DATA AVAILABILITY STATEMENT

The dataset used in this study is publicly available at https://zenodo.org/records/17993788.

ACKNOWLEDGEMENT

Tran Thu Minh was funded by the Master's and PhD Scholarship Programme of Vingroup Innovation Foundation (VINIF), under grant code VINIF.2024.ThS.68.

REFERENCES

[1] T. T. Tran, T. M. Tran, X. T. Nguyen, V. T. Nguyen, and B. T. Vu, "Durability and Strength of Reinforced Concrete Bridges Subject to Corrosion: Fuzzy Random and Probabilistic Analysis," *Nigerian Journal of Technological Development*, vol. 21, no. 4, pp. 85–96, Feb. 2025, https://doi.org/10.4314/njtd.v21i4.2593.

[2] H. T. Nguyen, B. Cosson, M.-F. Lacrampe, and T. A. Do, "Numerical Simulation of Reactive Polymer Flow During Rotational Molding using Smoothed Particle Hydrodynamics Method and Experimental Verification," *International Journal of Material Forming*, vol. 11, no. 4, pp. 583–592, July 2018, https://doi.org/10.1007/s12289-017-1367-2.

[3] T. T. Tran, T. M. Tran, X. T. Nguyen, D. H. Nguyen, B. T. Vu, and V. N. Vo, "Influences of Pre-Bending Load and Corrosion Degree of Reinforcement on the Loading Capacity of Concrete Beams," *Journal of the Mechanical Behavior of Materials*, vol. 31, no. 1, pp. 554–563, July 2022, https://doi.org/10.1515/jmbm-2022-0061.

[4] V. H. Hoang, T. A. Do, A. T. Tran, and X. H. Nguyen, "Flexural Capacity of Reinforced Concrete Slabs Retrofitted with Ultra-High-

Performance Concrete and Fiber-Reinforced Polymer," *Innovative Infrastructure Solutions*, vol. 9, no. 4, Apr. 2024, Art. no. 113, https://doi.org/10.1007/s41062-024-01410-y.

[5] B. Guo, X. Lin, Y. Wu, and L. Zhang, "Advanced Analytical Model and Reliability Analysis for Long-Term Deflection of FRP Reinforced Concrete Beams with Compression Yielding Mechanism," *Structures*, vol. 80, Oct. 2025, Art. no. 110130, https://doi.org/10.1016/j.istruc.2025.110130.

[6] M. Abdel-Jaber, R. Al-Nsour, and A. Ashteyat, "Flexural Strengthening and Rehabilitation of Continuous Reinforced Concrete Beams using BFRP Sheets: Experimental and Analytical Techniques," *Composites Part C: Open Access*, vol. 16, Mar. 2025, Art. no. 100556, https://doi.org/10.1016/j.jcomc.2024.100556.

[7] *Eurocode 2: Design of Concrete Structures - Part 1-1: General Rules and Rules for Buildings*, EN 1992-1-1, European Standardization Organizations, Brussels, Belgium, Dec. 2004.

[8] T. Y. Lin and N. H. Burns, *Design of Prestressed Concrete Structures*, 3rd ed. Hoboken, USA: John Wiley & Sons, Incorporated, 1981.

[9] M. N. Fardis, *Seismic Design, Assessment and Retrofitting of Concrete Buildings*, vol. 8. Dordrecht, Netherlands: Springer Netherlands, 2009.

[10] A. Ghali, A. M. Neville, and T. G. Brown, *Structural Analysis: A unified classical and matrix approach*, 6th ed. Boca Raton, FL, USA: CRC Press, 2017.

[11] J. Jia and Y. Li, "Deep Learning for Structural Health Monitoring: Data, Algorithms, Applications, Challenges, and Trends," *Sensors*, vol. 23, no. 21, Oct. 2023, Art. no. 8824, https://doi.org/10.3390/s23218824.

[12] T. Lou, S. M. R. Lopes, and A. V. Lopes, "Nonlinear and Time-Dependent Analysis of Continuous Unbonded Prestressed Concrete Beams," *Computers & Structures*, vol. 119, pp. 166–176, Apr. 2013, https://doi.org/10.1016/j.compstruc.2012.12.014.

[13] V. H. Hoang, N. L. Nguyen, T. T. Bui, and N. H. Tran, "A Two-Stage Method for Damage Detection in Z24 Bridge Based on K-nearest Neighbor and Artificial Neural Network," *Periodica Polytechnica Civil Engineering*, vol. 68, no. 3, pp. 892–902, Apr. 2024, https://doi.org/10.3311/PPci.23884.

[14] L. Nguyen-Ngoc, T. A. Do, V. H. Hoang, T. T. Hoang, and T. D. Tran, "Equivalent Convective Heat Transfer Coefficient for Boundary Conditions in Temperature Prediction of Early-Age Concrete Elements using FD and PSO," *KSCE Journal of Civil Engineering*, vol. 27, no. 6, pp. 2546–2558, June 2023, https://doi.org/10.1007/s12205-023-1116-7.

[15] H. Tran-Ngoc, Q. Nguyen-Huu, T. Nguyen-Chi, and T. Bui-Tien, "Enhancing Damage Detection in Truss Bridges Through Structural Stiffness Reduction using 1DCNN, BiLSTM, and Data Augmentation Techniques," *Structures*, vol. 68, Oct. 2024, Art. no. 107035, https://doi.org/10.1016/j.istruc.2024.107035.

[16] Q. N. Huu, L. N. Ngoc, T. B. Tien, H. T. Ngoc, H. N. Tran, and T. N. Xuan, "An Improved Artificial Rabbit Optimization for Structural Damage Identification," *Latin American Journal of Solids and Structures*, vol. 21, no. 1, 2024, Art. no. e523, https://doi.org/10.1590/1679-78257810.

[17] L. YiFei *et al.*, "Metamodel-Assisted Hybrid Optimization Strategy for Model Updating using Vibration Response Data," *Advances in Engineering Software*, vol. 185, Nov. 2023, Art. no. 103515, https://doi.org/10.1016/j.advengsoft.2023.103515.

[18] H. N. Tran, Q. H. Nguyen, and T. T. Bui, "Leveraging Physics-Based Optimization and Singular Value Decomposition for Enhanced Structural Damage Detection," *Engineering Computations*, June 2025, https://doi.org/10.1108/EC-07-2024-0675.

[19] H. Tran-Ngoc, T. Le-Xuan, S. Khatir, G. De Roeck, T. Bui-Tien, and M. Abdel Wahab, "A Promising Approach using Fibonacci Sequence-Based Optimization Algorithms and Advanced Computing," *Scientific Reports*, vol. 13, no. 1, Feb. 2023, Art. no. 3405, https://doi.org/10.1038/s41598-023-28367-9.

[20] A. Imam, F. Anifowose, and A. K. Azad, "Residual Strength of Corroded Reinforced Concrete Beams using an Adaptive Model Based on ANN," *International Journal of Concrete Structures and Materials*, vol. 9, no. 2, pp. 159–172, June 2015, https://doi.org/10.1007/s40069-015-0097-4.

[21] M. E. A. Ben Seghier, V. Plevris, and A. Malekjafarian, "Development of Hybrid Adaptive Neural Fuzzy Inference System-Based Evolutionary Algorithms for Flexural Capacity Prediction in Corroded Steel Reinforced Concrete Beam," *Arabian Journal for Science and Engineering*, vol. 48, no. 10, pp. 13147–13163, Oct. 2023, https://doi.org/10.1007/s13369-023-07708-w.

[22] Y. Yang, C. Zhou, and J. Peng, "Prediction of Flexural Capacity of Corroded Reinforced Concrete Beams by Physics-Informed Neural Network," *Case Studies in Construction Materials*, vol. 23, Dec. 2025, Art. no. e05475, https://doi.org/10.1016/j.cscm.2025.e05475.

[23] A. B. Malkawi, A. A. Yasin, and F. R. Maraqa, "ANN Prediction of Flexural Capacity of Lightweight Reinforced Concrete Beams with Tuff Aggregates," *Journal of Soft Computing in Civil Engineering*, vol. 10, no. 2, Art. no. 1931, 2026.

[24] *Standard for Testing Methods of Concrete Structures*, GB/T 50152-2012, Standardization Administration of China, Beijing, China, Aug. 2012.

[25] G. S. Fishman, *Monte Carlo: Concepts, Algorithms, and Applications*, 7th ed. New York City, NY, USA: Springer, 2008.

[26] S. S. Flayyih, F. H. Jasim, O. T. Nafe'e, and A. A. J. Jamel, "An Artificial Intelligence-Driven Evaluation of Scour Depth Around Bridge Piers," *Engineering, Technology & Applied Science Research*, vol. 15, no. 5, pp. 26310–26316, Oct. 2025, https://doi.org/10.48084/etasr.12240.

[27] T. M. Tran, "Synthetic Dataset for Prestressed Reinforced Concrete Beam Flexural Capacity Generated Using Monte Carlo Simulations." zenodo, Dec. 2025, [Online]. Available: https://zenodo.org/records/17993788.